

# The numerical study of the cavitation–structure interaction around 3D flexible hydrofoil

Hu Shi-liang, Chen Ying and Lu Chuan-jing

Department of Engineering Mechanics, Shanghai Jiao Tong University, No. 800 Dongchuan Road, Shanghai, China

E-mail: jerry542\_hu@hotmail.com

**Abstract.** The closely coupled approach combined the Finite Volume Method (FVM) solver and the Finite Element Method (FEM) solver is applied to simulation the cavitation–structure interaction of a 3D cantilevered flexible hydrofoil in water tunnel. In the cavitating flow, the elastic hydrofoil would deform or vibrate in bending and twisting mode. And the motion of the foil would affect the characteristics of the cavity and the hydrodynamic load on the foil in turn. With smaller cavitation numbers ( $\sigma_v=2.15$ ), the frequency spectrum of the lift on the foil would contain two frequencies which are associated to the cavity shedding and the first bend frequency of the hydrofoil. With larger cavitation number ( $\sigma_v=2.55$ ), the frequency of the lift is completely dominated by the natural frequency of the foil.

## 1. Introduction

Recently, hydrofoil blades of marine propellers and turbomachinery are being designed with light weight and thin profile to increase the efficiency. With such flexible structures, the fluid load would induce structure oscillation and inversely the time-space distribution of the flow would also be influenced by the structure motion. When the pressure on the suction side of foil drops down under the saturating vapor pressure of liquid, the cavitation occurs and the interaction between the cavitation and structure could not be ignored.

Although many efforts were made in fluid-structure interaction (FSI) for aerodynamics application, relatively few works show concern for hydro-elasticity. Amromin and Kovinskaya<sup>[1]</sup> analyzed the vibration of an 2D elastic wing with an attached cavity in a periodically perturbed flow. Campbell and Paterson<sup>[2]</sup> developed and implemented a FSI solver to model a quasi-steady problem of a single 3D foil vibration in water. Torre et al.<sup>[3]</sup> experimentally investigated the influence of leading edge cavitation and supercavitation on the added mass effects experienced by a 2D truncated hydrofoil. Young<sup>[4]</sup> presented a coupled Boundary Element Model (BEM) and Finite Element Method (FEM) approach to study the fluid structure interaction of flexible composite propellers in subcavitating and cavitating flows. Ducoin et al.<sup>[5]</sup> analyzed the structural response of a rectangular cantilevered flexible hydrofoil submitted to various flow regimes through the experiment carried out in a hydrodynamic tunnel.

In the present work, the cavitation–structure interaction effects on a 3D cantilevered flexible hydrofoil in the water tunnel are numerical investigated. The Reynolds-averages Navier-Stokes equations (RANS) for fluid domain are solved by the Finite Volume Method (FLUENT). The turbulence effect is modeled using the RNG  $k$ - $\varepsilon$  model, and the cavitating flow is computed using the cavitation model suggested by Zwart et al.<sup>[6]</sup>, in which a transport equation for the volume fraction of



vapor phase is calculated. The hydrofoil is treated as elastic body with small deformation and the damping effect is neglected. The material of hydrofoil is considered as isotropic. The structure domain is dispersed by the Finite Element Method (ANSYS). The coupled method between the fluid and structure solver is based on the closely coupled approach<sup>[7]</sup>.

## 2. Problem description

The fluid domain is 1m long and has a 0.192m square cross section, which is shown in figure 1. The hydrofoil is a NACA66 with a camber ratio of 2% and a relative thickness of 12%. The chord is  $c=0.15$  m and the span is  $b=0.191$  m. One end of the hydrofoil is fixed on the wall of the tunnel, and the other end is set free. The gap between the free end and the vertical wall is 1 mm. The angle between the chord and the horizontal coordinate  $X$  is defined as the attack angle  $\alpha$ . Point A is the leading point at free end of the hydrofoil, and the central axis  $S$  is located at  $x/c=0.5$ . The flexible hydrofoil has a Polyacetate (POM) material with  $\rho^s=1480$  kg/m<sup>3</sup>,  $E=3000$  MPa,  $\nu=0.35$ .

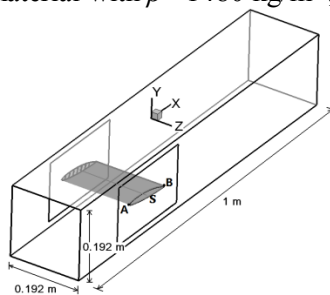


**Figure 1.** Geometric properties of fluid domain.

## 3. Result and discussion

The investigation of cavitation–structure interaction is carried out with the initial angle  $\alpha=8^\circ$  and  $Re=\rho^f U_\infty c/\mu^f=7.5 \times 10^5$ . Through decreasing the pressure  $p_\infty$  in the tunnel, five cases with the cavitation number  $\sigma_v=1.95, 2.15, 2.28, 2.55$  and  $2.80$  are simulated, where the  $\sigma_v$  is defined by:

$$\sigma_v = \frac{p_\infty - P_v}{1/2 \rho^f U_\infty^2} \quad (1)$$

Table 1 compares the maximum lift coefficient and the maximum cavity length on the rigid and flexible hydrofoil with different cavitation numbers. It is shown that the elasticity of the structure would promote the maximum cavity length and increase the extreme value of lift on the foil. Figure 2 indicates that the numerical results of the maximum displacement of point A versus the maximum length of cavity have the same trend as the experimental ones. The free end displacement would increase with the enlargement of the cavity on the hydrofoil. Figure 3 illustrates the maximum twist angle of the section along the span and the maximum vertical displacement of the axis S. The results show that the deformation of the flexible foil increases with the reduction of cavitation number, whereas the cavitation number almost has no influence on the deformation mode in these cases.

**Table 1.** The comparison of the maximum lift coefficient and the maximum cavity length between the rigid and flexible foil.

$\sigma_v$	$Cl_{\max}$		$(l_{\text{cav}})_{\max}$ (m)	
	Rigid foil	Flexible foil	Rigid foil	Flexible foil
1.95	1.310	1.391	0.0593	0.0615
2.15	1.271	1.343	0.0465	0.0486
2.28	1.262	1.304	0.0326	0.0347
2.55	1.151	1.179	0.0195	0.0214
2.80	1.098	1.101	0.0059	0.0059

### 3.1. $\sigma_v=2.15$

The time history of the lift coefficient and the displacement of point A for  $\sigma_v=2.15$  are shown in figure 4. It is presented that the variation of the lift and tip displacement has the same phase. Figure 5 gives the frequency spectrum of the lift for both rigid and flexible foil. It reveals that the spectrum of the rigid foil only has one main frequency (about 20Hz) related to the cloudy cavity shedding, while the spectrum of the flexible foil has two peaks and one of the peaks (about 42Hz) is quite close to the first bending frequency of the hydrofoil in water ( $f_1=43\text{Hz}$ ). Figure 6 and 7 compare the lift coefficient and the cavity length of the rigid and flexible foil in one period. In the ascent stage of lift ( $0 \sim 2/6T_0$ ), the flexible foil moves upward synchronously (seen in figure 4). The motion of foil restrain the development of the cavity on the suction side which leads to the lift on the flexible foil is relatively small. In the descend stage of lift ( $2/6T_0 \sim 4/6T_0$ ), the flexible foil moves downward. The growth rate of the cavity on the flexible foil is quicker than that of rigid foil and the lift on the flexible foil is much larger. At about  $4/6T_0$ , the partial cavity on both rigid and flexible foil is cut by the reentrant jet and sheds from the leading edge.

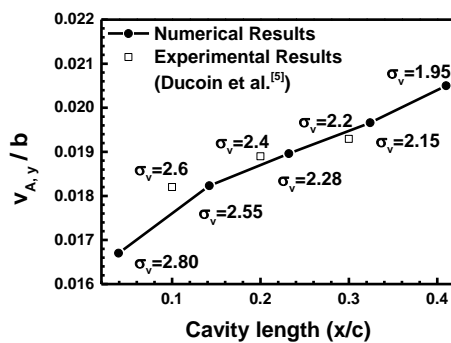


**Figure 2.** Maximum displacement of point A versus maximum cavity length.

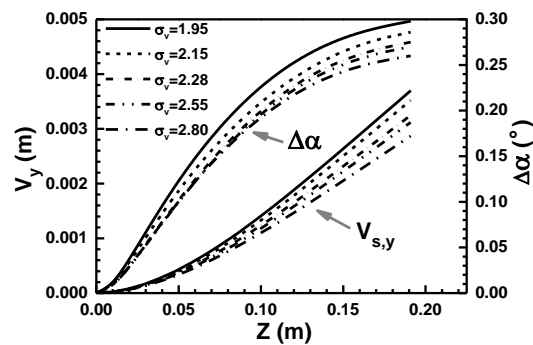


**Figure 3.** The maximum twist angle and the maximum displacement of axis S for different cavitation number.

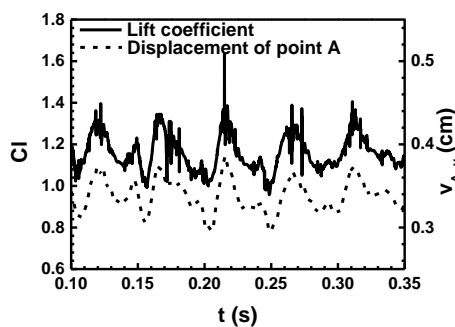


**Figure 4.** The time history of the lift coefficient on the hydrofoil and the displacement of point A for  $\sigma_v=2.15$

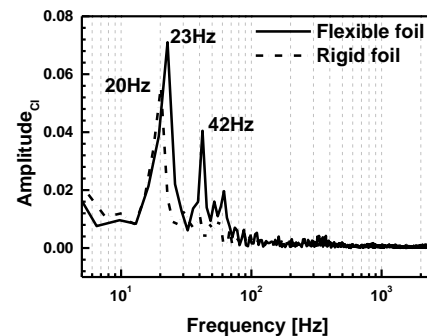


**Figure 5.** The comparison of the lift coefficient spectrum for  $\sigma_v=2.15$ .

### 3.2. $\sigma_v=2.55$

The time history of the lift coefficient on the rigid and flexible foil for  $\sigma_v=2.55$  (figure 8) displays that the vibration of the foil does change the regime of cavitating flow. The lift coefficient on the rigid foil has no obvious regularity and the amplitude of the fluctuation is narrow. However, on the deformable foil, the lift coefficient oscillates periodically with large amplitude. The spectrum (figure 9) shows that the single frequency peak of the lift coefficient on the flexible foil is 40Hz ( $f_1=43\text{Hz}$ ), which indicates that the movement of the foil domains the unsteady characteristic of the flow field with  $\sigma_v=2.55$ . In

figure 10, the vortex structure at the middle section of the fluid field ( $z/b=0.5$ ) is visualized based on the Q-criterion. The influence of the structure motion on the flow regime could be clearly seen.

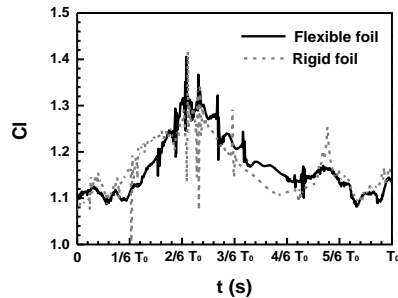


**Figure 6.** The lift coefficient in one cycle  $T_0$ .

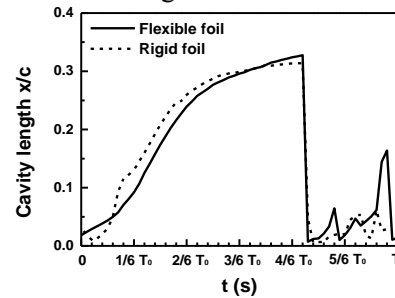


**Figure 7.** The cavity length in one cycle  $T_0$ .

#### 4. Conclusion

In the present work, the closely coupling approach is selected as coupling strategy in the numerical modeling. And the cavitation–structure interaction for a cantilevered 3D flexible hydrofoil in the water tunnel is studied. The results show that the hydrodynamic loads would cause the bending and twisting deformation of the foil and the vibration of the foil would also affect the regime of the cavitating flow.

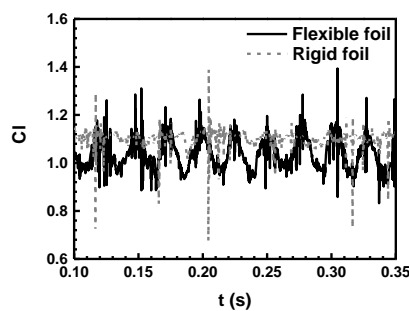


**Figure 8.** The lift coefficient of the flexible and rigid foil for  $\sigma_v=2.55$ .

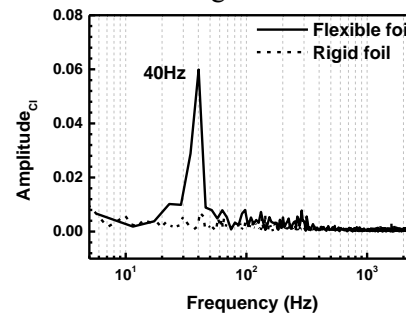


**Figure 9.** The comparison of the lift coefficient spectrum for  $\sigma_v=2.55$ .

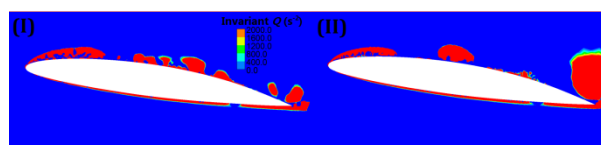


**Figure 10.** The vortex structure (based on the Q-criterion) at the middle section of the fluid field ( $z/b=0.5$ ) with  $\sigma_v=2.55$ . (I) Rigid foil. (II) Flexible foil

#### Acknowledgments

This project is supported by the National Nature Science Foundation of China (Grant No. 11472174). Its financial support is gratefully acknowledged.

#### References

- [1] Amromin E and Kovinskaya S 2000 *J. Fluid. Struct.* **14** 735–751.
- [2] Campbell R L and Paterson E G 2011 *J. Fluid. Struct.* **27**, 1376–91.
- [3] De La Torre O, Escaler X, Egusquiza E and Farhat M 2013 *J. Fluid. Struct.* **39**, 173–187
- [4] Young Y L 2008 *J. Fluid. Struct.* **24**, 799–818.
- [5] Ducoin A, Astolfi A J and Sigrist J F 2012 *Eur. J. Mech. B-Fluid* **36** 63–74.
- [6] Zwart P J, Gerber A G and Belamri T 2004 *5th Int. Conf. Multiphase Flow (Japan: Yokohama)*.
- [7] Lian Y, Shyy W, Ifju P and Verron E 2002 *AIAA Paper* **2972** 2492–94.